International Journal of Engineering Research & Technology (IJERT)
ISSN: 2278-0181
Vol. 2 Issue 9, September - 2013

# Numerical Study of Double Diffusive Mixed Convection with Variable Fluid Properties

Nalinakshi N.
*Department of Mathematics, Atria Institute of Technology, Bangalore – 560 024, Karnataka India*

Dinesh P.A.
*Department of Mathematics, M. S. Ramaiah Institute of Technology, Bangalore – 560 054, India*

Chandrashekar D.V.
*Department of Mathematics, Vivekananda Institute of Technology, Bangalore – 560 074, India*

## Abstract

*A Numerical approach has been carried out for the study of Double Diffusion and Mixed convection from a vertical heated plate embedded in a Newtonian fluid saturated sparsely packed porous medium by considering the variation of permeability, porosity, thermal conductivity and solutal diffusivity. The boundary layer flow in the porous medium is governed by Lapwood-Brinkman extended Darcy model. An Interesting instability results when the density of the fluid depends on two opposing gradients that is the double diffusion. Similarity transformations are employed and the resulting ordinary differential equations are solved using shooting technique with Runge–Kutta-Fehlberg scheme to obtain velocity, temperature and concentration distributions. The features of fluid flow, heat and mass transfer characteristics are analyzed by plotting the graphs and the physical aspects are discussed in detail to interpret the effect of various significant parameters of the problem. The results obtained show that the impact of buoyancy ratio parameter N, Prandtl number Pr, Schmidt number Sc and other parameters plays an important role in the fluid flow through porous medium. Further, the obtained results under the limiting conditions were found to be in good agreement with the existing results.*

## "1. Introduction"

Double diffusive transport phenomenon has encouraged the interest due to their applications in both industrial and agricultural fields like solar power collectors, packed bed catalytic reactors, migration of moisture in fibrous insulation, heat exchangers, cooling of radioactive waste containers, polluting transport in saturated soils, grain storage installation, underground spread of pollutants, food processing and others. Literatures are found relative to thermal and solutal natural convection whose studies are relative either to a semi-infinite medium limited by a flat plate or to confined – geometry Cavities or enclosures with walls subjected to heat and mass fluxes. Double Diffusive natural convection in packed beds do not take into account water evaporation or condensation rate within grains but assume that grains are inert, this was motivated by Zili-Ghediri et al[1] to consider the water evaporation and condensation within grains. Subsequently, Chen [2] made a study on combined heat and mass transfer in MHD free convection from a vertical surface with ohmic heating and viscous dissipation. Mucoglu and Chen [3] have studied the mixed convection flow over an inclined surface for both the assisting and the opposing buoyancy forces. Seddeek [4] finds that the fluid viscosity is assumed to vary as an inverse linear function of temperature in the study of Thermal-diffusion and diffusion-thermo effects on mixed free –forced convective flow and mass transfer over an accelerating surface with a heat source in the presence of suction and blowing in the case of variable viscosity. Ahmed et al [5] have studied the effects of chemical reaction in presence of a heat source with MHD mixed convection and mass transfer from an infinite vertical porous plate. Mixed convection boundary layer flow on an impermeable vertical surface embedded in a saturated porous has been treated by Kairi [6]. Murti et al [7] analyzed the effects of radiation, chemical reaction and double dispersion on heat and mass transfer in non – Darcy free convective flow. The extension of this work including inertial effects was made by

Awad et al [8] using the modified Darcy-Brinkman model to investigate double diffusive convection in a Maxwell fluid in the presence of Dufour and Soret effects in a highly porous medium. Wang and Tan [9] studied stability analysis of double-diffusive convection of Maxwell fluid in a porous medium heated from below and also they extended their study in the stability analysis of soret-driven double diffusive convection of Maxwell fluid in a porous medium. Sri Hari Babu and Ramana Reddy [10] studied Mass transfer effects on MHD mixed convective flow from a vertical surface with ohmic heating and viscous dissipation by using multi parameter perturbation technique. In most of these studies the effects are described by Fourier and Fick's law. Ferdows et al [11] analyzed the effect of Variable Viscosity in double diffusion problem of MHD from a porous boundary with Internal Heat Generation. Alam et al [12] made a numerical study of combined free-forced convection and mass transfer flow past a vertical porous plate in porous medium with heat generation and thermal diffusion. Kesavaiah et al [13] studied the effects of the chemical reaction and radiation absorption on an unsteady MHD convective heat and mass transfer flow past a semi-infinite vertical permeable moving plate embedded in a porous medium with heat source and suction. However, for the study of flow through porous media due to double diffusion with lateral mass flux have important engineering applications in a petroleum industry, purification of crude oil, polymer technology, groundwater hydrology, etc.

All the above mentioned studies treat the permeability, conductivity or thermal resistance and solutal diffusivity of the medium as constants. However, porosity measurements by Shwartz and Smith [14] and Benenati and Brosilow [15] show that porosity is not constant but varies from the wall to the interior due to which permeability also varies. Chandrashekar et al [16,17] has incorporated the variable permeability to study the flow past and through a porous medium and have shown that the variation of porosity and permeability has greater influence on velocity distribution and on heat transfer. Mohommadien and El-shaer [18] analyzed influence of variable permeability on combined free and forced convection flow past a semi-infinite vertical plate in a saturated porous media incorporating the variation of permeability and thermal conductivity. Nalinakshi et al [19] found numerical solutions for heat transfer from a vertical heated plate embedded in a Newtonian fluid sparsely packed porous medium considering the variable fluid properties with the influence of inertial parameter. Nalinakshi et al [20], further analysed the MHD effect on Mixed convection heat transfer from a vertical heated plate by considering the variable fluid properties.

The aim of the present investigation is to study numerically and systematically the effect of inertial terms on double diffusion and combined free and forced convection heat and mass transfer past a semi-infinite vertical plate embedded in a saturated porous medium with variable permeability, porosity, thermal conductivity and solutal diffusivity. The boundary layer flow in the porous medium is governed by Lapwood- Brinkmann extended Darcy model. In this analysis, coupled non-linear partial differential equation, governing the problem are first reduced by a similarity transformation to the ordinary differential equation and then the resultant boundary value problem is converted into the system of seven simultaneous equations of first order for seven unknowns, then these equations are solved numerically by shooting technique with Runge-Kutta method to obtain horizontal velocity, temperature and concentration profiles for various values of physical parameters. The results obtained from the present numerical computation under limiting condition agree well with the existing ones and thereby verifies the accuracy of the method used.

## "2. Mathematical Formulation"

A two-dimensional steady combined free-forced convective and mass transfer flow of a viscous, incompressible fluid over an isothermal semi-infinite vertical porous flat plate embedded in a sparsely packed porous medium of variable porosity, permeability, thermal conductivity and variable diffusivity is considered (see Fig.1). The x-coordinate is measured along the plate from its leading edge, and y-coordinate normal to it. Let $U_o$ be the velocity of the fluid in the upward direction and the gravitational field, g, is acting in the downward direction. The surface of the plate is maintained at a uniform constant temperature $T_w$ and a uniform constant concentration $C_w$, of a fluid, which are higher than the free stream values existing far from the plate $\left(i.e., T_w > T_\infty, C_w > C_\infty\right)$. It is also assumed that the free stream velocity $U_0$, parallel to the vertical plate, is constant. Then under the boundary layer and Boussinesq's approximations, the equations governing the conservation of mass, momentum, energy and concentration are given by:

$$\frac{\partial u}{\partial x}+\frac{\partial v}{\partial y}=0 \tag{1}$$

$$\rho\left(u\frac{\partial u}{\partial x}+v\frac{\partial u}{\partial y}\right)=\rho g\beta_T\left(T-T_\infty\right)-\rho g\beta_C\left(C-C_\infty\right) +\bar{\mu}\frac{\partial^2 u}{\partial y^2}+\frac{\mu\varepsilon(y)}{k(y)}\left(U_0-u\right) \tag{2}$$

$$u\frac{\partial T}{\partial x}+v\frac{\partial T}{\partial y}=\frac{\partial}{\partial y}\left(\alpha(y)\frac{\partial T}{\partial y}\right)+\frac{\bar{\mu}}{\rho C_p}\left(\frac{\partial u}{\partial y}\right)^2 \qquad (3)$$

$$u\frac{\partial C}{\partial x}+v\frac{\partial C}{\partial y}=\frac{\partial}{\partial y}\left(\gamma(y)\frac{\partial C}{\partial y}\right) \qquad (4)$$

where u and v are the velocity components along the x and y directions respectively, T is the temperature of the fluid, $T_\infty$ is the ambient temperature, C is the species concentration ,$C_\infty$ is the species concentration at $\infty$, $\rho$ is the fluid density, g is the acceleration due to gravity, $\bar{\mu}$ is the effective viscosity of the fluid, $\mu$ is the fluid viscosity, $k(y)$ is the variable permeability of the porous medium, $\varepsilon(y)$ is the porosity of the saturated porous medium, $\alpha(y)$ is the variable effective thermal diffusivity of the medium, $\gamma(y)$ is the variable effective solutal diffusivity of the medium, $C_p$ is the specific heat at constant pressure, $\beta_T$ is the coefficient of volume expansion, $\beta_C$ is the volumetric coefficient of expansion with species concentration .

The above governing equations need to be solved subject to the following boundary conditions on velocity, temperature and concentration fields:

$$u=0, v=0, T=T_w, C=C_w \text{ at } y=0 \qquad (5)$$

$$u=U_o, v=0, T=T_\infty, C=C_\infty \text{ as } y\to\infty \qquad (6)$$

We now introduce the following dimensionless variables f , θ, $\phi$ as well as the similarity variable η (see Mohammadein and El-Shaer[18]):

$$\eta=\left(\frac{y}{x}\right)\left(\frac{U_o x}{v}\right)^{1/2}, \quad \psi=\sqrt{vU_o x}\, f(\eta),$$

$$\theta=\frac{T-T_\infty}{T_w-T_\infty}, \quad \phi=\frac{C-C_\infty}{C_w-C_\infty}. \qquad (7)$$

The stream function $\psi(x,y)$ is defined by $u=\frac{\partial\psi}{\partial y}$, $v=-\frac{\partial\psi}{\partial x}$, such that the continuity equation (1) is satisfied automatically and the velocity components are given by

$$u=U_o f'(\eta), \quad v=-\frac{1}{2}\sqrt{\frac{vU_o}{x}}\left(f(\eta)-\eta f'(\eta)\right) \qquad (8)$$

where, a prime represents differentiation with respect to $\eta$ , $T_w$ is the plate temperature and $C_w$ is the plate concentration.

Following Chandrasekhar and Namboodiri[17], the variable permeability $k(\eta)$, the variable porosity $\varepsilon(\eta)$ and variable effective thermal diffusivity $\alpha(\eta)$ are given by

$$k(\eta)=k_o\left(1+de^{-\eta}\right) \qquad (9)$$

$$\varepsilon(\eta)=\varepsilon_o\left(1+d^*e^{-\eta}\right) \qquad (10)$$

$$\alpha(\eta)=\alpha_o[\varepsilon_o\left(1+d^*e^{-\eta}\right)+\sigma^*\{1-\varepsilon_o\left(1+d^*e^{-\eta}\right)\}] \qquad (11)$$

and the variable solutal diffusivity $\gamma(\eta)$ is given by

$$\gamma(\eta)=\gamma_o[\varepsilon_o\left(1+d^*e^{-\eta}\right)+\gamma^*\{1-\varepsilon_o\left(1+d^*e^{-\eta}\right)\}] \qquad (12)$$

where $k_o$, $\varepsilon_o$, $\alpha_o$ and $\gamma_o$ are the permeability, porosity, thermal conductivity and solutal diffusivity at the edge of the boundary layer respectively, $\sigma^*$ is the ratio of the thermal conductivity of solid to the conductivity of the fluid, $\gamma^*$ is the ratio of the thermal diffusivity of solid to the diffusivity of the fluid, $d$ and $d^*$ are treated as constants having values 3.0 and 1.5 respectively for variable permeability and d = $d^*$= 0 for uniform permeability.

Substituting (7) and (8) in Equations (2), (3) and (4), we get the following transformed equations

$$f'''+\frac{1}{2}ff''+\frac{Gr}{\mathrm{Re}^2}(\theta-N\phi)+\frac{\alpha^*\left(1+d^*e^{-\eta}\right)}{\sigma\,\mathrm{Re}\left(1+de^{-\eta}\right)}\left(1-f'\right)=0 \qquad (13)$$

$$\theta''=-\frac{\left(\tfrac{1}{2}\right)\mathrm{Pr}\,\theta' f+\mathrm{Pr}\,Ef''^2+\varepsilon_o d^*e^{-\eta}\left(\sigma^*-1\right)\theta'}{\varepsilon_o+\sigma^*(1-\varepsilon_o)+\varepsilon_o d^*e^{-\eta}\left(1-\sigma^*\right)} \qquad (14)$$

$$\phi''=-\frac{\left(\tfrac{1}{2}\right)Sc\,\phi' f+\varepsilon_o d^*e^{-\eta}\left(\gamma^*-1\right)\phi'}{\varepsilon_o+\gamma^*(1-\varepsilon_o)+\varepsilon_o d^*e^{-\eta}\left(1-\gamma^*\right)} \qquad (15)$$

where, $\mathrm{Pr}=\bar{\mu}/\rho\alpha_o$ is the Prandtl number, $Sc=\bar{\mu}/\rho\gamma_o$ is the Schmidt number, $\alpha^*=\mu/\bar{\mu}$ is the ratio of viscosities, $N=\frac{\beta_C(C_w-C_\infty)}{\beta_T(T_w-T_\infty)}$ is the Buoyancy ratio, $E=U_o^2/C_p(T_w-T_\infty)$ is the Eckert number, $\sigma=k_o/x^2\varepsilon_o$ is the local permeability parameter, $\mathrm{Re}=U_o x/v$ is the local Reynolds number and $Gr_T=g\beta_T(T_w-T_\infty)x^3/v^2$ is the thermal Grashof number, $Gr_c=g\beta_C(C_w-C_\infty)x^3/v^2$ is the solutal Grashof number, $Ri=Gr/\mathrm{Re}^2$ is the Richardson number. Here $Gr_T=Gr_C$ is considered.

The transformed boundary conditions are

$$f=0,\ f'=0,\ \theta=1,\ \phi=1 \quad \text{at} \quad \eta=0 \qquad (16)$$

$$f'=1,\ \theta=0,\ \phi=0 \quad \text{as} \quad \eta\to\infty \qquad (17)$$

Once the velocity, temperature and concentration distributions are known, the skin friction and the rate of heat and mass transfer can be calculated respectively by

$$\tau = -f''(0)\big/\sqrt{\mathrm{Re}}\,,\ Nu = -\sqrt{\mathrm{Re}}\,\theta'(0)$$
$$Sh = -\sqrt{\mathrm{Re}}\,\phi'(0) \qquad (18)$$

where $\tau$ is the skin friction , Nu is the Nusselt number and Sh is the Sherwood number.

## "3.Numerical Method"

Equations (13),(14) and (15) constitute a highly non-linear coupled boundary value problem (BVP) of third and second order respectively. An improved numerical scheme involving shooting technique with Runge-Kutta-Fehlberg method is developed to solve the resulting nonlinear BVP. Thus, the coupled nonlinear boundary value problem of third-order in f and second-order in $\theta$ and $\phi$ has been reduced to a system of seven simultaneous equations of first-order for seven unknowns as follows–(see Vajravelu[21]):

$$f_1' = f_2$$
$$f_2' = f_3$$
$$f_3' = -\frac{1}{2} f_1 f_3 - \frac{Gr}{\mathrm{Re}^2}\left(f_4 - N f_6\right) - \frac{\alpha^*(1+d^* e^{-\eta})}{\sigma\,\mathrm{Re}(1+de^{-\eta})}(1-f_2)$$
$$f_4' = f_5$$
$$f_5' = -\frac{(1/2)\Pr f_1 f_5 + \Pr E f_3^2 + \varepsilon_o d^* e^{-\eta}(\sigma^* - 1) f_5}{\varepsilon_o + \sigma^*(1-\varepsilon_o) + \varepsilon_o d^* e^{-\eta}(1-\sigma^*)}$$
$$f_6' = f_7$$
$$f_7' = -\frac{(1/2) Sc f_1 f_7 + \varepsilon_o d^* e^{-\eta}(\sigma^* - 1) f_7}{\varepsilon_o + \sigma^*(1-\varepsilon_o) + \varepsilon_o d^* e^{-\eta}(1-\sigma^*)} \qquad (19)$$

where $f_1 = f,\ f_2 = f',\ f_3 = f'',\ f_4 = \theta,\ f_5 = \theta'$, $f_6 = \phi,\ f_7 = \phi'$ and a prime denotes differentiation with respect to $\eta$.

The boundary conditions now become

$$f_1 = 0,\ f_2 = 0,\ f_4 = 1,\ f_6 = 1 \quad \text{at} \quad \eta = 0 \qquad (20)$$
$$f_2 = 1,\ f_4 = 0,\ f_6 = 0 \quad \text{as} \quad \eta \to \infty \qquad (21)$$

## "4. Results and Discussion"

The system of first-order differential equations (19)-(21) are solved numerically using shooting technique with Runge-Kutta-Fehlberg method. In order to know the accuracy of the method used, computed values of $f''(0)$, $\theta'(0)$ and $\phi'(0)$ were obtained for buoyancy ratio $N = 0$ for the variable permeability (d=3.0, $d^*$=1.5) case and uniform permeability (d=0.0, d*=0.0) case. The values are tabulated in Table 1 and Table 2 for $\varepsilon_o = 0.4, Ec = 0.1, \Pr = 0.71, \mathrm{Sc} = 0.22$ with selected values of $Gr/\mathrm{Re}^2$ ,$\sigma^*$ and $\alpha^*/\sigma\,\mathrm{Re}$ for uniform permeability and variable permeability respectively. Mohammedein and El-shaer [18] have analyzed the heat transfer problem with variable permeability. The computed values here for heat and mass transfer are well agreed with the values of Mohammadein and El-Shaer [18] with only the heat transfer. Thus the present results are more accurate compared to their results.

As a result of the numerical calculations, the dimensionless velocity, temperature and concentration distributions for the flow under consideration are obtained and their behaviour have been discussed for variations in the governing parameters namely, the buoyancy ratio N, $Gr/\mathrm{Re}^2$, $\alpha^*/\sigma\mathrm{Re}$, and $\sigma^*$ with the fixed prandtl number Pr, Eckert number Ec, Schmidt number Sc, porosity of the saturated porous medium at the edge of the boundary layer $\varepsilon_0$ in both UP and VP cases.

Figure 2 depicts the typical velocity distributions in the boundary layer for various values of buoyancy ratio N for Variable permeability (VP) case. It is observed that, increase in the value of buoyancy ratio N , leads to an increase in the velocity profile within the boundary layer (and the boundary layer increases with decrease in the value of N) near the porous plate and decays smoothly to the free stream velocity. Figure 3 shows the temperature profiles for various values of buoyancy ratio N for VP case. From this figure it is observed that the temperature profile decreases for all values of N within the boundary layer. The rate of cooling is faster for large values of N. Figure 4 illustrates the concentration profiles for various values of N for VP case. It is observed that concentration profiles decreases for all values of N within the boundary layer.

Figure 5 shows the variation of velocity distributions for various values of the parameter $Gr/\mathrm{Re}^2$ (here the thermal buoyancy force and solutal buoyancy force is taken as equal) for both the cases of UP and VP. The relative importance of free and forced convection for determining the combined flow is shown by the magnitude of $Gr/\mathrm{Re}^2$. It is observed that increase in the value of $Gr/\mathrm{Re}^2$ increases the velocity distribution for both UP and VP cases considered which is very significant for higher value in the boundary layer. For particular value of $Gr/\mathrm{Re}^2$ the velocity profile is found to be lighter for VP as compared to UP case. It is clearly seen in the velocity profiles that, effect of VP is more prominent when $Gr/\mathrm{Re}^2$=2.0 and boundary layer decreases with increase in the value of $Gr/\mathrm{Re}^2$. This is due to the fact that in the process of cooling the heated plate, the free convection currents are carried away from the plate to the free stream and as the free stream is in the upward direction, the free convection currents induce the mean velocity to increase. The increase in buoyancy effects and hence increases in the value of $Gr/\mathrm{Re}^2$ results in causing more induced flow along the plate in the vertical direction which is reflected by the increase in the fluid velocity. Hence the velocity profiles become sharply peaked near the wall indicating the influence of free convection in modifying the flow field with the increase in the value $Gr/\mathrm{Re}^2$.

Figure 6 illustrates the temperature distributions for various values of $Gr/\mathrm{Re}^2$ for both the cases UP and VP. Here temperature profile decreases in the boundary layer for all the values of $Gr/\mathrm{Re}^2$ for the cases. The profiles are always less for VP case compared to UP case, as the effect of buoyancy parameter $Gr/\mathrm{Re}^2$ is to increase the surface heat and enhancement in the flow velocity increases the porous surface. It shows that increase in the buoyancy parameter $Gr/\mathrm{Re}^2$ decreases the thermal boundary layer thickness, which in turn increases the wall temperature gradient producing the increase in the surface heat transfer rate.

Figure 7 shows the concentration profiles for various values of $Gr/\mathrm{Re}^2$ for both the VP and UP case. We can observe that there is a decrease in concentration distribution as the magnitude of $Gr/\mathrm{Re}^2$ increases, for higher value that is $Gr/\mathrm{Re}^2$ =2.0 the concentration profile decreases steeply for both UP and VP cases.

Figure 8 shows the variations of velocity profiles for various values of $\alpha^*/\sigma\mathrm{Re}$ for both the UP and VP cases. It can be observed that the velocity profile increases with increase in the value of. Velocity profiles for VP case are less compa $\alpha^*/\sigma\mathrm{Re}$ red to UP case. Figure 9 shows the temperature profiles for various values of $\alpha^*/\sigma\mathrm{Re}$ for both UP and VP cases. It is observed that there is a decrease in the temperature distributions with the increase in the value of $\alpha^*/\sigma\mathrm{Re}$. The boundary layer is less for VP compared to UP case.

Figure 10 depicts the concentration profiles for different values of $\alpha^*/\sigma\mathrm{Re}$ for both the UP and VP case. Increase in the values of $\alpha^*/\sigma\mathrm{Re}$, we observe that there is a decrease in the concentration profiles for both UP and VP case.

Figure 11 illustrates the variation of velocity profiles for different values of Prandtl numbers (Pr =0.71, 3.0, 7.0 and 10) for variable permeability case. It is seen that velocity profiles decreases as the prandtl number increases, more significant in the middle of the boundary layer, boundary layer decreases with the decrease in the value of Pr. Figure 12 depicts the temperature profiles for various values of Prandtl number for both UP and VP cases. The temperature profiles decreases as the prandtl number increases, for higher prandtl number there is a steep decrease in the boundary layer for both UP and VP cases.

Figure 13 shows the concentration profiles for different values of Schmidt number for UP and VP cases. Increase in the Schmidt number there is a decrease in concentration profile and the boundary layer is little high for VP case compared to those of UP case.

## "5. Conclusions"

In this paper, a numerical model is developed for double diffusive mixed convection past a semi infinite vertical heated plate in a saturated porous medium by considering the variable fluid properties like variable permeability, porosity, thermal conductivity and solutal diffusivity. The boundary layer flow in the porous medium is governed by Lapwood- Brinkman extended Darcy model. Using the similarity variables, the governing equations are transformed into a set of highly coupled non linear ordinary differential equations. These equations are then solved numerically by Runge-Kutta method with shooting technique. The computed results are presented to illustrate the details of flow and heat and mass transfer characteristics and also their dependence on the physical parameters, the following conclusions are drawn:

1. Buoyancy ratio N is to increase the velocity distribution significantly, decrease in the temperature and concentration distribution for Variable Permeability (VP) case.
2. Increasing the Buoyancy force, the number $Gr/\mathrm{Re}^2$ increases which lead to increase the velocity closer to the vertical heated plate, and decrease in the parameter $Gr/\mathrm{Re}^2$ enhances the temperature and concentration in the boundary layer for both cases. The temperature and concentration profiles for VP are always less compared to UP.
3. With an increase of $\alpha^*/\sigma\mathrm{Re}$ the velocity profile increases, decrease in the parameter $\alpha*/\sigma\mathrm{Re}$ enhances the temperature and concentration in the boundary layer for both cases. The profiles are less for VP compared to UP.

4. With an increase of Pr the velocity profile decreases, whereas it enhances the temperature and increase of Sc it enhances the concentration.

**Table 1:** Results for $f''(0), -\theta'(0)$ and $-\phi'(0)$ for

| N | $\sigma^*$ $\gamma^*$ | $Gr/Re^2$ | $\alpha^*/\sigma Re$ | Uniform permeability (UP) | | |
|---|---|---|---|---|---|---|
| | | | | $f''(0)$ | $-\theta'(0)$ | $-\phi'(0)$ |
| 0 | 2 | 0 | 0 | 0.424675 | 0.294532 | 0.276531 |
| | | | 0.1 | 0.454523 | 0.324515 | 0.300516 |
| | | | 0.5 | 0.667584 | 0.456321 | 0.426181 |
| | | 0.2 | 0 | 0.625782 | 0.384321 | 0.374532 |
| | | | 0.1 | 0.662551 | 0.454517 | 0.434505 |
| | | | 0.5 | 0.800523 | 0.549051 | 0.545516 |
| | | 2 | 0 | 0.757323 | 0.424563 | 0.400612 |
| | | | 0.1 | 0.900055 | 0.495601 | 0.474551 |
| | | | 0.5 | 1.303581 | 0.556517 | 0.546512 |
| | 4 | 0.2 | 0.1 | 0.854532 | 0.554573 | 0.530071 |
| 1 | 2 | 0 | 0 | 0.498321 | 0.387562 | 0.395781 |
| | | | 0.1 | 0.527584 | 0.459872 | 0.456891 |
| | | | 0.5 | 0.724509 | 0.567801 | 0.558914 |
| | | 0.2 | 0 | 0.574321 | 0.425671 | 0.400561 |
| | | | 0.1 | 0.685432 | 0.486791 | 0.482672 |
| | | | 0.5 | 0.902553 | 0.552754 | 0.532753 |
| | | 2 | 0 | 0.765672 | 0.457863 | 0.438751 |
| | | | 0.1 | 1.503804 | 0.546709 | 0.536802 |
| | | | 0.5 | 1.734282 | 0.558003 | 0.546003 |
| | 4 | 0.2 | 0.1 | 0.912354 | 0.523456 | 0.500512 |
| 5 | 2 | 0.2 | 0.1 | 0.945432 | 0.627875 | 0.601053 |
| | | | 0.5 | 1.205673 | 0.657892 | 0.650001 |
| 10 | 2 | 0.2 | 0.1 | 1.354322 | 0.634561 | 0.629324 |
| | | | 0.5 | 1.500345 | 0.675641 | 0.667891 |

Pr = 0.71, Sc=0.22, Ec = 0.1, $\varepsilon_0 = 0.4$ for Uniform Permeability (UP) case.



**“6. Acknowledgements”**

The authors are grateful to the Research Centre M S Ramaiah Institute of Technology, Atria Institute of Technology, Vivekananda Institute of Technology, for all the support and also the financial support from VTU research scheme project.

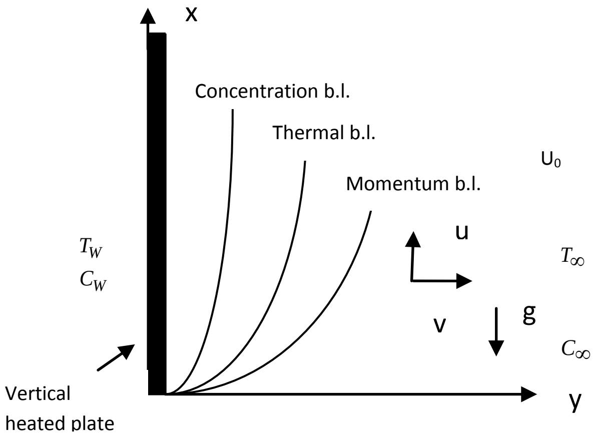


**Figure 1:** Physical model and coordinate system

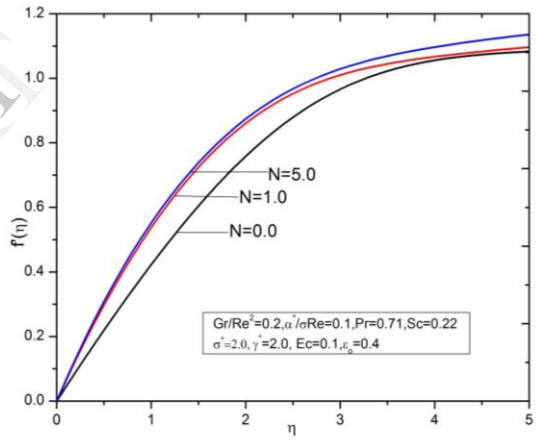


**Figure 2:** Velocity profiles for different values of N for Variable permeability (VP) case

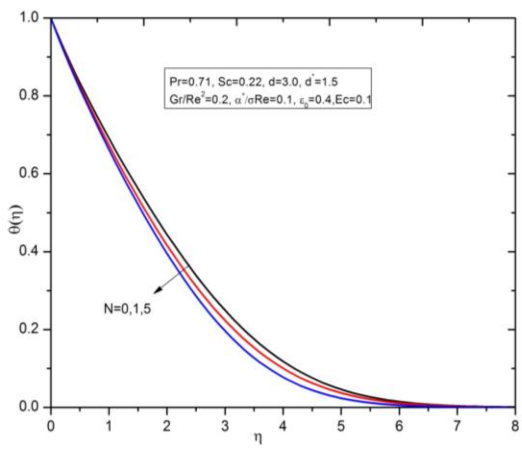

**Figure 3:** Temperature profiles for different values of N for Variable permeability (VP) case

| N | $\sigma^*$ $\gamma^*$ | $Gr/\mathrm{Re}^2$ | $\alpha^*/\sigma\mathrm{Re}$ | Variable permeability (VP) | | |
|---|---|---|---|---|---|---|
| | | | | $f''(0)$ | $-\theta'(0)$ | $-\phi'(0)$ |
| 0 | 2 | 0 | 0 | 0.478651 | 0.375601 | 0.358902 |
| | | | 0.1 | 0.495604 | 0.394281 | 0.390054 |
| | | | 0.5 | 0.800501 | 0.496752 | 0.490023 |
| | | 0.2 | 0 | 0.700503 | 0.445632 | 0.440021 |
| | | | 0.1 | 0.867502 | 0.526501 | 0.520001 |
| | | | 0.5 | 0.873564 | 0.568901 | 0.560123 |
| | | 2 | 0 | 0.800541 | 0.456531 | 0.451452 |
| | | | 0.1 | 1.005652 | 0.556781 | 0.550041 |
| | | | 0.5 | 1.536721 | 0.657891 | 0.650034 |
| | 4 | 0.2 | 0.1 | 0.900456 | 0.694353 | 0.681345 |
| 1 | 2 | 0 | 0 | 0.699851 | 0.556754 | 0.549802 |
| | | | 0.1 | 0.723456 | 0.587501 | 0.569003 |
| | | | 0.5 | 0.772101 | 0.658512 | 0.641238 |
| | | 0.2 | 0 | 0.758901 | 0.561754 | 0.551154 |
| | | | 0.1 | 0.900567 | 0.600451 | 0.594331 |
| | | | 0.5 | 0.978901 | 0.651789 | 0.631456 |
| | | 2 | 0 | 0.889503 | 0.581452 | 0.577232 |
| | | | 0.1 | 1.600141 | 0.605678 | 0.600012 |
| | | | 0.5 | 2.134282 | 0.623456 | 0.619872 |
| | 4 | 0.2 | 0.1 | 0.996754 | 0.589341 | 0.561132 |
| 5 | 2 | 0.2 | 0.1 | 1.036789 | 0.675431 | 0.650034 |
| | | | 0.5 | 1.456782 | 0.681432 | 0.670134 |
| 10 | 2 | 0.2 | 0.1 | 1.558978 | 0.643451 | 0.631342 |
| | | | 0.5 | 1.778956 | 0.68132 | 0.679432 |

**Table 2:** Results for $f''(0)$, $-\theta'(0)$ and $-\phi'(0)$ for Pr = 0.71, Sc=0.22, Ec = 0.1, $\varepsilon_0 = 0.4$, for variable permeability (VP) case.

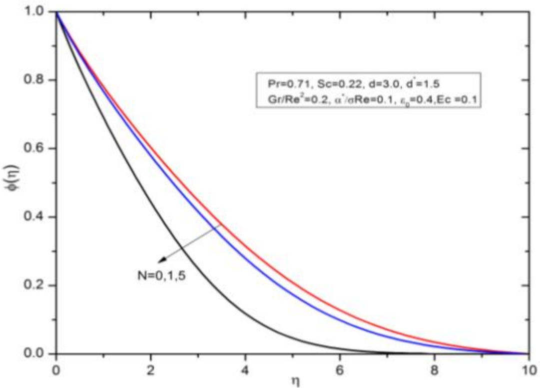


**Figure 4:** Concentration profiles for different values of N for Variable permeability (VP) case

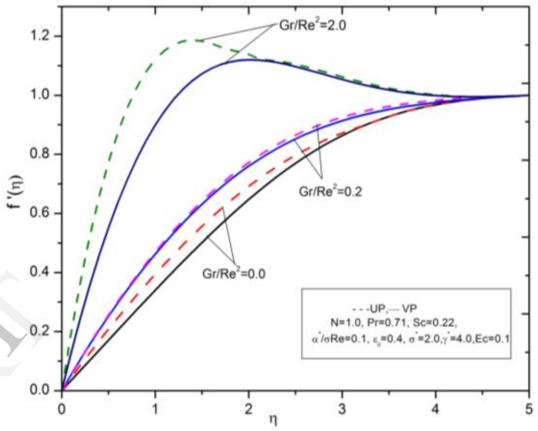


**Figure 5:** Velocity profiles for different values of $Gr/\mathrm{Re}^2$ for both UP and VP cases

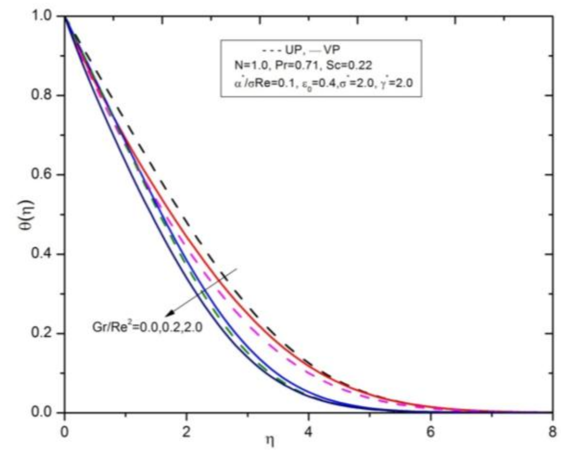


**Figure 6:** Temperature profiles for various values of $Gr/\mathrm{Re}^2$ for both UP and VP cases

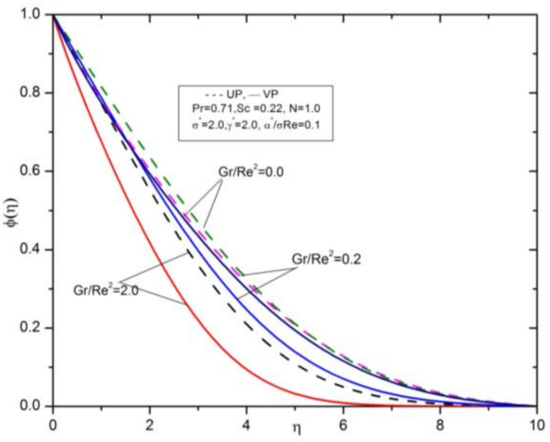


**Figure 7:** Concentration profiles for various values of $Gr/\mathrm{Re}^2$ for both UP and VP Case

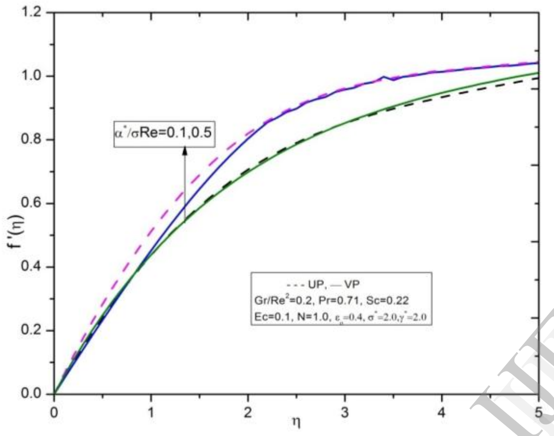


**Figure 8:** Velocity profiles for different values of $\alpha^*/\sigma \mathrm{Re}$ for both UP and VP cases

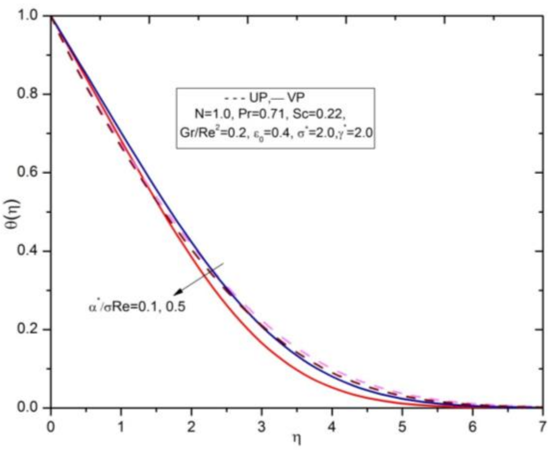


**Figure 9:** Temperature profiles for various values $\alpha^*/\sigma \mathrm{Re}$ for both UP and VP cases

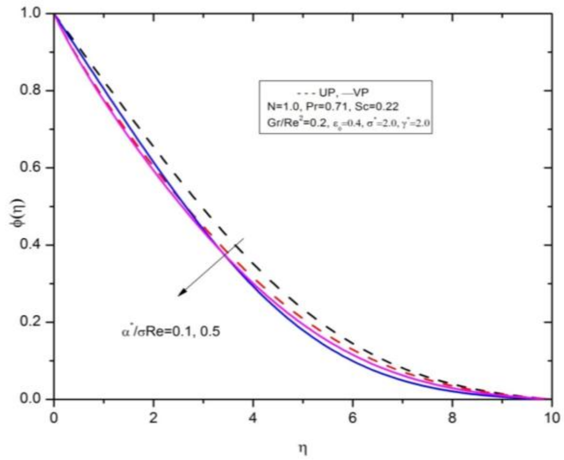


**Figure 10:** Concentration profiles for various values of $\alpha^*/\sigma \mathrm{Re}$ for both UP and VP case

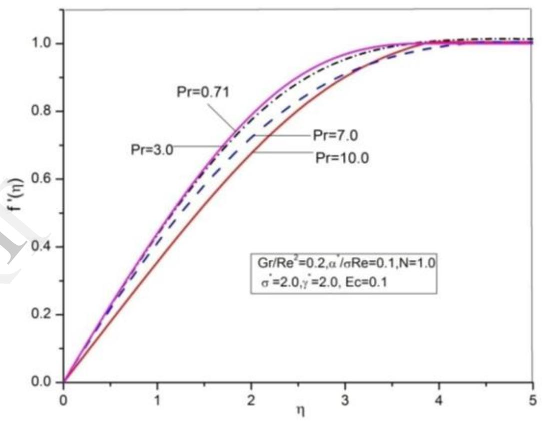


**Figure 11:** Velocity profiles for various values of Prandtl number for VP Case

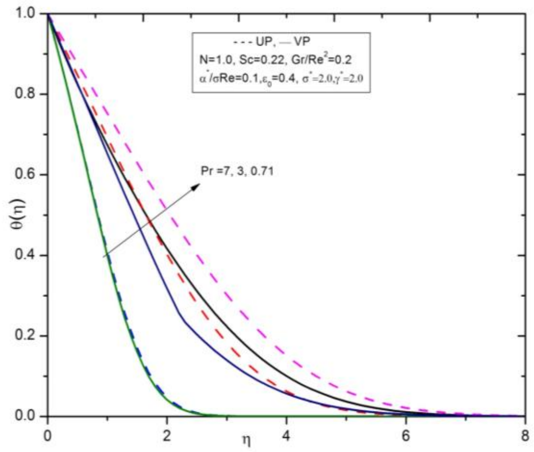


**Figure 12:** Temperature profiles for various values of Prandtl number for both UP and VP cases

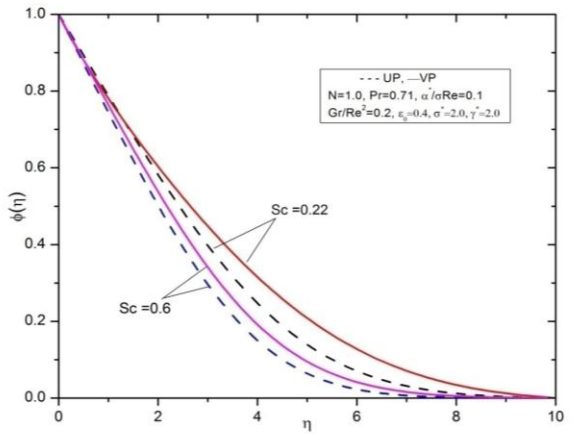


**Figure 13:** Concentration profiles for different values of Schmidt number for UP and VP case

## References


[1] L. Zili-Ghedira, K. Slimi, and S. Ben Nasrallah, "Double diffusive natural convection in a cylinder filled with moist porous grains and exposed to a constant wall heat flux", *Journal of Porous Media*, 6(2), (2003), pp. 123-136.

[2] C. H. Chen, "Combined heat and mass transfer in MHD free convection from a vertical surface with ohmic heating and viscous dissipation", *Int. J Engg. Sci*, 42(7), (2004), pp. 699-713.

[3] A. Mucoglu, T. S. Chen, Wave instability of mixed convection flow along a vertical flat plate. *Num. Heat Transfer I*, 1(2), (1978), pp. 267-283.

[4] M. A. Seddeek, "Thermal-diffusion and diffusion-thermo effects on mixed free-forced convective flow and mass transfer over an accelerating surface with a heat source in the presence of suction and blowing in the case of variable viscosity", *Acta Mechanica*, 172, (2004), pp. 83-94.

[5] N. Ahmed, D. Sarma, H. Deka, "MHD mixed convection and mass transfer from an infinite vertical porous plate with chemical reaction in presence of a heat source", *Applied Mathematical Science, 6(21)*, (2012), pp. 1011-1020.

[6] R. R. Kairi, P. V. S. N. Murthy, "The effects of double dispersion on natural convection heat and mass transfer in a non-Newtonian fluid saturated non-Darcy porous medium", *Transport Porous Media*, 76, (2009), pp. 377-390.

[7] A.S.N. Murti, D.R.V.S.R.K. Sastry, P. K. Kameswaran, T. Poorna Kantha, "Effects of mixed convection and double dispersion on semi infinite vertical plate in presence of radiation", *World Academy of Sci. Engg. Tech.*, 60, (2011), pp. 1232-1239.

[8] F. G. Awad, P. Sibanda, S. S. Motsa "On the linear stability analysis of a maxwell fluid with double-diffusive convection", *Applied Mathematical Modelling*, 34, (2010), pp. 3509-3517.

[9] Wenchang Tan, Shaowei Wang, "Stability analysis of double-diffusive convection of maxwell fluid in a porous medium heated from below", *Physics Letters A 372*, (2008), pp.3046-3050.

[10] V. Sri Hari Babu, G. V. Ramana Reddy, "Mass transfer effects on MHD mixed convective flow from a vertical surface with ohmic heating and viscous dissipation", *Advances in Applied Science Reasearch*, 2(4), (2011), pp. 138-146.

[11] M. Ferdows, M. Z. I. Bangalee, J. C. Crepeau, M. A. Seddeek, "The effect of variable viscosity in double diffusion problem of MHD from a porous boundary with Internal heat generation", *Progress in Computational Fluid Dynamic*, 11(1), (2011), pp. 54-65.

[12] M. S. Alam, M. M. Rahman, M. A. Samad, "Numerical study of the combined free-forced convection and mass transfer flow past a vertical porous plate in a porous medium with heat generation and thermal Diffusion", *Nonlinear Analysis: Modelling and Control*, 11(4), (2006), pp. 331-343.

[13] D. Kesavaiah, P. V. Satyanarayana, S. Venkataramana, "Effects of the chemical reaction and radiation absorption on an unsteady MHD convective heat and mass transfer flow past a semi-infinite vertical permeable moving plate embedded in a porous medium with heat source and suction", *Int. J Appl. Math and Mech.*, 7(1), (2011), pp. 52-69.

[14] C. E. Schwartz, J. M. Smith, "Flow distribution in packed beds", *Ind. Eng. Chem.*, 45, (1953), pp. 1209-1218.

[15] R. F. Benanati, C. B. Brosilow (1962). "Void Fraction distribution in beds of spheres", *AIChe. J.* 8, (1962), pp. 359-361.

[16] B. C. Chandrasekhara, P. M. S. Namboodiri, & A. R. Hanumanthappa, "Similarity solutions of buoyancy induced flows in a saturated porous medium adjacent to impermeable horizontal surfaces". *Warme Stoffubertrag*, 18, (1984), pp.17-23.

[17] B. C. Chandrasekhara, P. M. S. Namboodiri, "Influence of variable permeability on combined vertical surfaces in porous medium", *Int. J. Heat Mass Transfer*, 28 (1985), pp. 199-206.

[18] A. A. Mohammadein, N. A. El-Shaer, "Influence of variable permeability on combined free and forced convection flow past a semi – infinite vertical plate in a saturated porous medium", *Heat Mass Transfer*, 40, (2004), pp. 341-346.

[19] N. Nalinakshi, P. A. Dinesh, I. S. Shivakumara and D. V. Chandrashekar, "Numerical solution for mixed convection heat transfer from a vertical heated plate embedded in a sparsely packed porous medium", *J. Mapana* 10(2), (2011), pp. 37-53.

[20] N. Nalinakshi, P. A. Dinesh, and D. V. Chandrashekar, "Effects of Variable fluid properties and MHD on Mixed convection heat transfer from a vertical heated plate embedded in a sparsely packed porous medium", *IOSR Journal of Mathematics*, vol 7(1), (2013), pp. 20-31.

[21] K. Vajravelu, "Viscous flow over a nonlinear stretching sheet" *Applied Math. Computation*, 124, (2001), pp. 281 - 288.